Solar System Research, Vol. 34, No. 5, 2000, pp. 390–397. Translated from Astronomicheskii Vestnik, Vol. 34, No. 5, 2000, pp. 432–440.

Morphological Analysis of the Cratering of the South Pole–Aitken Basin on the Moon

Zh. F. Rodionova and E. A. Kozlova
Sternberg Astronomical Institute, Universitetskii pr. 13, Moscow, 119899 Russia
Received February 24, 1999; in final form, November 15, 1999

Abstract—Morphological features of craters in the South Pole–Aitken Basin are studied. Craters in the basin are compared to craters located in highland and mare regions. In comparison studies, the following morphological features were considered: (1) the degree of rim degradation; the presence of (2) terraces and faults, (3) hills, peaks, and ridges, (4) fissures and chains of small craters, (5) lava on the crater floor; (6) the character of the floor; and (7) the presence of ray systems. In the basin 3.8 million km^2 in area, 1538 craters of 10 km in diameter or larger are found. Craters in the South Pole–Aitken Basin are found to be less degraded than those in the mare region. Additionally, terraces on the inner slopes of craters in the basin are less degraded, and more faults are observed in the craters in the highland region. The craters in the three regions studied are similar in the presence of peaks and hills, while the density of craters with fissures and chains of small craters on the floor are greater in the mare region. No craters with ray systems are found in the basin. The South Pole–Aitken Basin is assumed to have formed late in the period of heavy bombardment.

INTRODUCTION

Previous studies of the morphology of lunar craters, mainly the youngest formations with prominent rims, revealed a correlation between the morphological features of such craters and their sizes (Basilevsky *et al.*, 1983; Florensky *et al.*, 1976, 1979; Hartmann, 1972). However, craters with prominent rims comprise less than 20% of all the lunar craters. Using the Morphological Catalogue of Lunar Craters created by Rodionova *et al.* (1987), which summarizes the coordinates, sizes, and main features of craters with diameters from 10 to 600 km, one can study the features of lunar cratering including craters with rims degraded to various degrees. The catalog was used for estimating the distribution of craters by morphological features both for the whole Moon and for individual lunar regions (Khramchikhin, 1994; Rodionova *et al.*, 1989a; Rodionova and Khramchikhin, 1996).

Morphological features of craters (the degree of rim degradation, the presence of peaks, ridges, fissures, chains of small craters, lava on the crater floor, terraces on inner slopes) depend on the size and composition of the impactor, its velocity, and the angle of incidence, as well as on the crater age and, most likely, the nature of the surface on which the crater is formed. Such features as faults and hills on the crater floor (by a fault we mean a part of the inner-slope material that has fallen on the crater floor) are secondary, since they appeared, most likely, as a result of crater degradation.

According to the degree of degradation, all the craters included in the catalog were divided into five classes: from class 1 (youngest, deepest craters) to class 5 (oldest, most destroyed craters).

Analysis of this data base (Rodionova *et al.*, 1989a) shows that the mean density of lunar craters of 10 km in diameter or larger is 393 per 1 million km^2, with 442 and 73 craters per 1 million km^2 for highland and mare regions, respectively. The formations from 10 to 19 km in diameter comprise 59% of all the craters studied; the craters from 20 to 39 km in diameter, 27%; and craters larger than 40 km in diameter, only 14%. Class 1 craters represent 19% of the total crater population; class 2 and class 3 craters, 27% each; class 4 craters, 21%; and class 5 craters, only 6% of the lunar craters. Class 1 craters were formed after the period of heavy bombardment. The global features of the distribution of craters into morphological classes are clearly seen on maps, where the density of craters of a given class (number of craters per 1 million km^2) is shown by isolines (Rodionova *et al.*, 1989b). Analysis of these maps revealed that the density of central-peak craters is maximum in the neighborhood of crater Einstein, the density of craters with ridges on the floor peaks in the regions northeast of Mare Moscoviense, craters with hills on the floor are clustered around Mare Orientale, and the maximum density of craters with fissures and chains of small craters is observed north of Mare Orientale, in the western margin of Oceanus Procellarum. The crater density in large basins, such as Mare Orientale, Mare Moscoviense, the Korolev Basin, and others, is about the same as that in maria on the nearside. The South Pole–Aitken Basin exhibits a higher crater density.

In this work, we focus on studying the morphology of craters in the giant South Pole–Aitken Basin on the lunar farside and its comparison with other equal-area lunar regions: a highland region on the nearside and a mare region including Mare Imbrium and some por-

0038-0946/00/3405-0390$25.00 © 2000 MAIK “Nauka / Interperiodica”

tions of Oceanus Procellarum and other maria. The area of each region is 3.8 million km^2. Thus, we considered about 30% of the lunar surface and examined more than 3700 craters. For comparison, we selected the highland region located near the center of the nearside in the southern hemisphere, because the South Pole–Aitken Basin is also placed in the southern hemisphere, near the center of the farside. The mare region selected for reference is the only continuous mare region unbroken by highlands.

DESCRIPTION OF SELECTED REGIONS

The *Clementine* altimetry data have confirmed the existence of a giant impact depression in the south portion of the lunar farside. This depression was first found on photographic images by the *Zond-6* and *Zond-8* spacecraft (Rodionov *et al.*, 1971, 1976). Topographic profiles of this basin were obtained by the laser altimeters aboard the *Apollo 15* and *Apollo 16* spacecraft. This structure is the greatest topographic formation on the Moon and the largest and deepest impact basin known in the Solar System. The basin was named according to its south (South Pole) and north (Aitken) boundaries. The South Pole–Aitken Basin displays a two-ring structure with a central depression about 2000 km in diameter and a rim about 2500 km in diameter. The basin depth is about 13 km from the rim to the floor. The South Pole–Aitken Basin is assumed to have formed between 4.3 and 3.9 billion years ago, in the earliest stage of lunar history, and to be one of the oldest structures on the lunar surface (Spudis *et al.*, 1994; Shoemaker *et al.*, 1994). However, Leikin and Sanovich (1985) speculated earlier that this basin is the youngest lunar depression with the least modified macrostructure.

The South Pole–Aitken Basin is abundant in craters including very large formations greater than 300 km in diameter: craters Planck, Poincare, Apollo, and Schrödinger and Mare Ingenii, which can be classified as basins according to their sizes (Fig. 1a). We found 1538 craters greater than 10 km in diameter. The density of craters in the South Pole–Aitken Basin, 405 craters per 1 million km^2, is close to the mean crater density of the lunar highlands, 442 craters per 1 million km^2 (Rodionova *et al.*, 1989a).

The *Lunar Prospector* data indicate that the KREEP-rich materials (materials containing high concentrations of potassium, rare-earth elements, and phosphorus) are clustered around the Mare Imbrium rims on the nearside and in the South Pole–Aitken Basin on the farside, whereas the highland regions exhibit low or usual KREEP concentrations. The large amount of KREEP-rich rocks was likely excavated onto the surface during impacts, which produced the Mare Imbrium Basin and the South Pole–Aitken Basin, or was formed as a result of mare basaltic volcanism. In addition, the data obtained using the gamma spectrometer aboard *Lunar Prospector* show that the Fe-rich

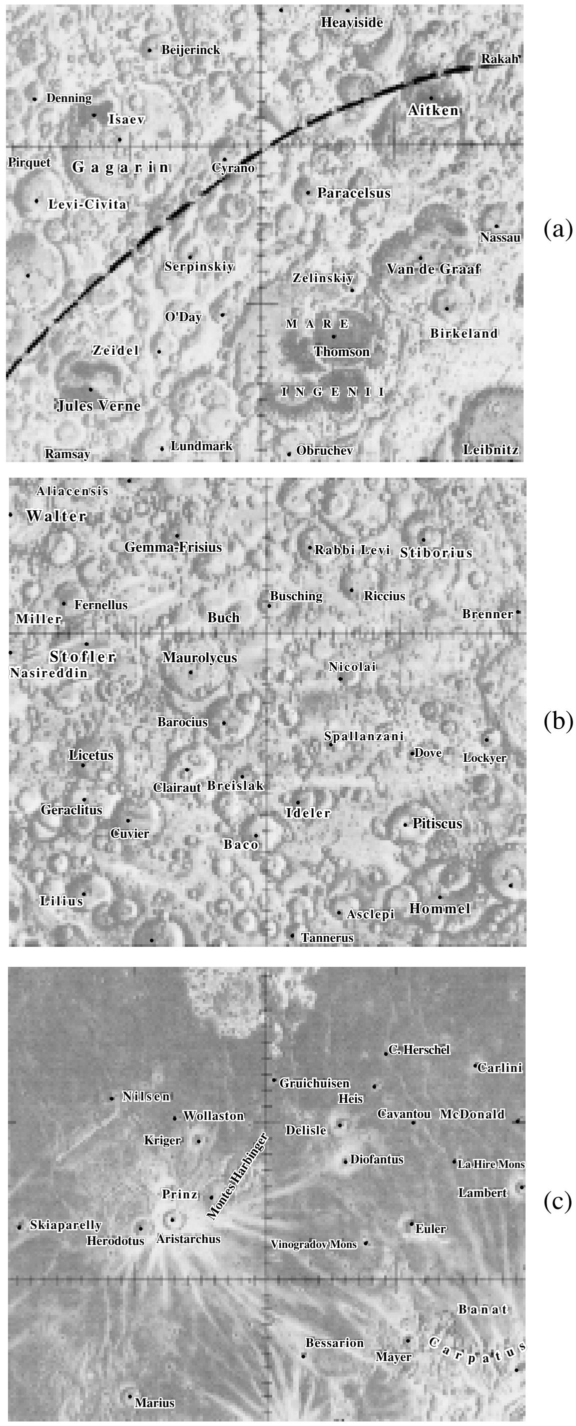

Fig. 1. Fragments of the lunar regions studied: (a) the South Pole–Aitken Basin (1130 x 980 km in area), (b) highland (900 x 915 km in area), and (c) mare (1130 x 980 km in area).

materials are mainly located in the mare regions on the lunar nearside, which is in good agreement with the previous data by *Clementine*. Strong magnetic fields in the South Pole–Aitken Basin, which are antipodal to Mare Imbrium and Mare Serenitatis, were revealed

Notation of the morphological features in the catalog

Feature	Meaning	Designation in the catalog	Feature	Meaning	Designation in the catalog
Degree of rim degradation	highly pronounced	1		one ridge	A
	pronounced	2		one ridge and one hill	B
	smoothed	3		one ridge and many hills	C
	degraded	4		one ridge and one peak	D
	ruin	5		one ridge and many peaks	E
Terraces and faults	no terraces	0	Fissures and chains of small craters	not attributed	0
	unclear	1		unclear	1
	one terrace	2		one chain	2
	one fault	3		many chains	3
	one terrace and one fault	4		one fissure	4
	many terraces	5		one chain and one fissure	5
	many terraces and faults	6		many fissures	6
Outer rim	no wall	0		one chain and many fissures	7
	unclear	1	Character of the crater floor	unclear	1
	wall	2		flat	2
	thick wall	3		rough	3
Peaks and hills	not attributed	0	Lavas on the crater floor	no lavas	0
	unclear	1		unclear	1
Ridges	one hill	2		partly flooded by lavas	2
	many hills	3		completely flooded by lavas	3
	one peak	4	Ray system	ray system	1
	one peak and one hill	5		unclear	2
	one peak and many hills	6		not attributed	3
	many peaks	7	Local terrain	plain	1
	many peaks and one hill	8		highland	2
	many peaks and hills	9		transition zone	3

with the magnetometer mounted aboard *Lunar Prospector*. These fields are sufficiently strong to produce the thinnest magnetosphere known in the Solar System (Binder, 1998).

The highlands are the oldest regions of the lunar crust. Their near-surface layer down to several kilometers in depth is composed by breccias—lithified ejecta of large craters. Some of the highland rocks solidified 4.4–4.6 billion years ago. The surface of the highlands is heavily cratered (Fig. 1b). Studies of highland rocks showed that they were heated to high temperatures about 3.9–4.0 billion years ago (Wilhelms, 1987), late in the period of heavy bombardment. A burst of bombardment with large, basin-forming bodies probably took place at this time. Falls of such celestial bodies resulted in the formation of the above-mentioned giant depressions—basins. Many of them have now been destroyed and are discovered only by altimetry data.

For comparison, we chose the highland region placed between 20° and 90°S and between 0° and 110°E. Large craters (e.g., Petavius, Boussingault) also occur in this region; however, their sizes are less than 200 km. The Tycho rays, Mountain Altai, Vallis Snellius, Vallis Rheita, and Vallis Palitzsch intersect this highland region. The total number of craters in the considered region is 1898. The mean crater density in this region, 487 craters per 1 million km^2, is 20% higher than that in the South Pole–Aitken Basin.

The mare region chosen for reference consists of Oceanus Procellarum, Mare Imbrium, and some areas of Mare Nubium and Mare Humorum. In this region, there are 270 craters greater than 10 km in diameter, including craters Aristarchus, Kepler, Copernicus, Eratosthenes, and others. Thus, the mean density of craters in the mare region is only 71 craters per 1 million km^2 or about 18% of the mean crater density in the South Pole–Aitken Basin (Fig. 1c).

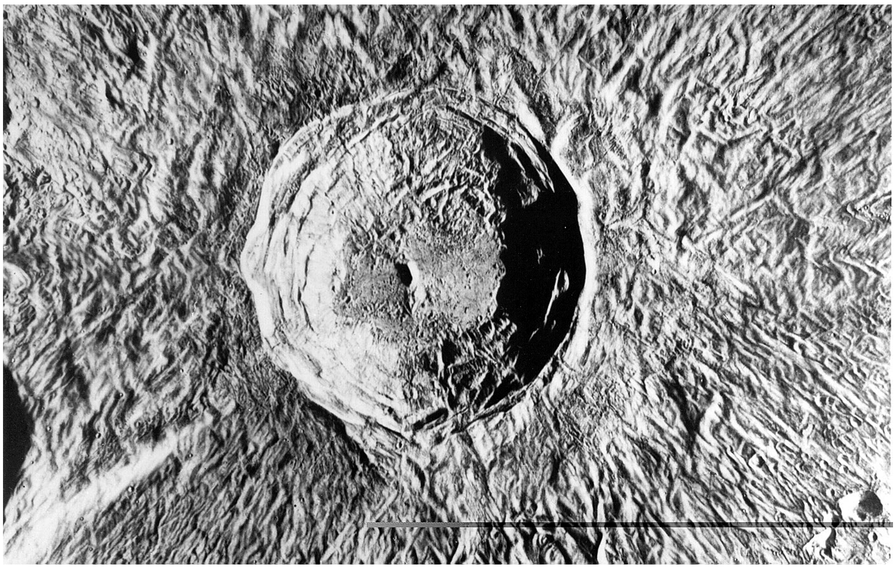

Fig. 2. Crater Aristarchus (108 × 69 km in area). A fragment of artistic shading of the relief made by cartographer Wayne Kaempfe.

SOURCE DATA FOR MORPHOLOGICAL ANALYSIS

In this work, we used The Morphological Catalogue of Lunar Craters (Rodionova *et al.*, 1987) compiled at the Sternberg State Astronomical Institute in collaboration with the Joint Institute for Nuclear Research (Dubna, Russia). This catalog contains coordinates, sizes, and nine major morphological features (see table) for 15000 craters greater than 10 km in diameter located both on the nearside and the farside of the Moon.

The morphological catalog has the following structure: the crater number, latitude (first three figures, south and north latitude are marked *S* and *N*, respectively), longitude (four figures), diameter in km, and main morphological features. Coordinates are given with an accuracy of 0.1°. Morphological characteristics and subcharacteristics are numbered according to the table. For instance, crater Aristarchus located in the mare region (Fig. 2) has coordinates 23.9°N, 312.5°E, a diameter of 42 km, a highly preserved rim, many terraces, a thick outer wall, many peaks, one chain of small craters, a rough floor, no lava on the floor, and a ray system. In the catalog, Aristarchus is represented as N2393125 42 153723022, where the last nine figures designate the morphological features in the order they are listed in the table.

Files containing information about craters located in the three selected regions were generated with the use of the program for sampling craters from the catalog, which was elaborated by S. G. Pugacheva (Sternberg State Astronomical Institute). Based on these files, we prepared tables that summarize data according to the morphological features under consideration.

COMPARISON OF MORPHOLOGICAL FEATURES OF CRATERS LOCATED IN THE SOUTH POLE–AITKEN BASIN, HIGHLAND REGION, AND MARE REGION

We used seven morphological characteristics to compare craters located in the South Pole–Aitken Basin with craters in the highland and mare regions: (*1*) the degree of rim degradation; the presence of (*2*) terraces and faults, (*3*) peaks, hills and ridges, (*4*) fissures and chains of small craters, (*5*) lavas on the crater floor; (*6*) the character of the floor; and (7) the presence of ray systems. Since the areas of the selected regions are equal, we can compare both the total numbers of craters and the crater densities (number of craters per 1 million km^2).

A comparative study of the morphological characteristics of craters revealed the following features:

Degree of rim degradation. The distributions of craters according to morphological classes for the highland region and the South Pole–Aitken Basin are similar; however, the craters with preserved rims are most abundant in the basin, whereas the highland region is dominated by craters with smoothed rims. The number of class 1 craters (highly pronounced rim) with diameters from 10 to 320 km in the basin is 28% greater than that in the highland region, and the number of class 2 craters (pronounced rim) in the basin is 8% greater than that in the highland region. The total number of class 3 craters (smoothed rim) in the highland region is 33% greater than the number of class 3 craters in the basin. The numbers of class 4 craters (degraded rim) and class 5 craters (ruins) in the highland region are 34 and 63% greater than those in the basin, respectively.

Thus, craters in the highland regions are more degraded than craters in the South Pole–Aitken Basin,

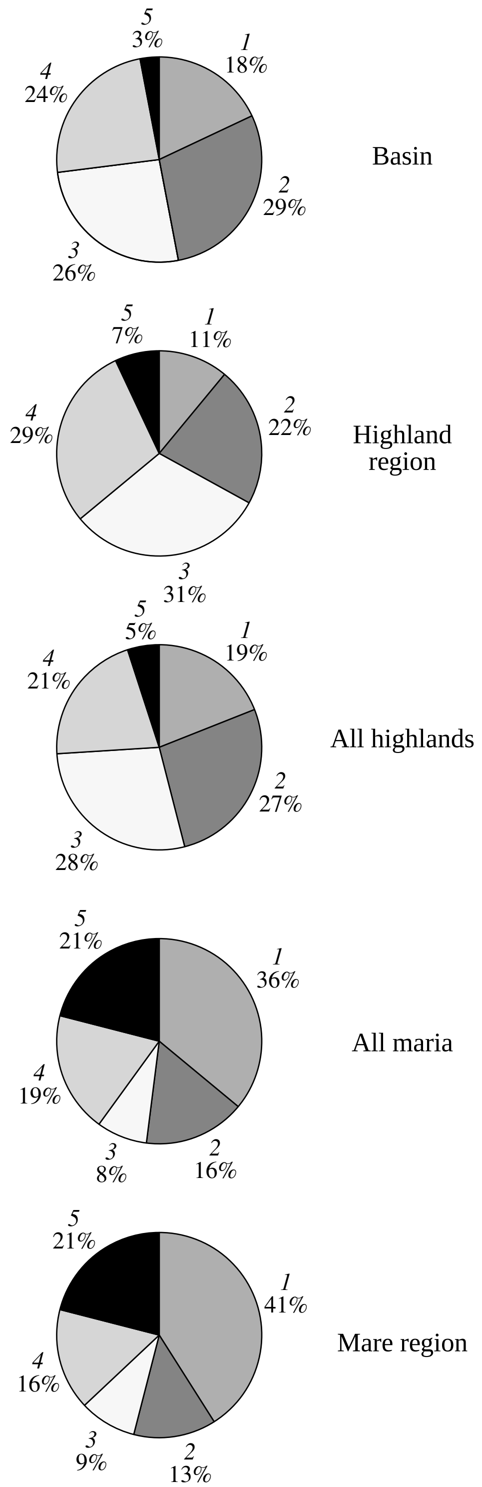

Fig. 3. Diagrams of distributions of craters by morphological classes: (*1*) highly pronounced rim, (*2*) pronounced rim, (*3*) smoothed rim, (*4*) degraded rim, and (*5*) ruin.

because the highland region is older. However, the distribution of craters in the basin according to the first characteristic is almost the same as the mean distribution for the lunar highlands, whereas the distribution of craters in the selected highland region differs drastically from the mean distribution (Fig. 3). Therefore, we assumed that processes that caused stronger crater degradation proceeded in the southern portion of the nearside highland.

For the mare region, the distribution of craters by morphological classes is quite different. The total number of class 1 craters in the basin is 62% greater than that in the mare region, and the total number of class 2 and class 3 craters in the basin is 93% higher than the numbers of such craters in the mare region. The number of class 4 craters in the basin is greater by 89%. The South Pole–Aitken Basin is abundant in class 5 craters of 10–20 km in diameter, whereas most of the class 5 craters in the mare region are from 20 to 320 km in diameter.

In the mare region, class 1 and class 5 craters are most abundant, with the maximum number class 1, whereas the basin is dominated by craters of classes 2–4, and class 2 craters are the most frequent. These distinctions are explained by the fact that many of the craters in the mare region were additionally destroyed during the period of basaltic volcanism. Less destroyed craters date to the later period and represent younger structures (Figs. 3, 4).

Terraces and faults. The distributions of craters according to the degree of inner-slope degradation for the South Pole–Aitken Basin and the highland region are also similar: craters with one terrace or one terrace and one fault dominate, whereas craters with many terraces or craters with many terraces and one fault are absent.

The number of type 1 craters (one terrace) in the basin is 28% greater than that in the highland region. The number of type 2 craters (one fault) in the highland region is 38% greater than the number of type 2 craters in the basin. Type 3 craters (one terrace and one fault) are also predominant in the highland region. Type 4 craters (many terraces) and type 5 craters (many terraces and faults) are absent both in the highland region and the basin.

For the mare region, the distribution of craters is different: the region is dominated by craters with faults, craters with one terrace and one fault and craters with many terraces are numerous, craters with many terraces and faults are moderate in number, and craters with one terrace are few.

For the mare region, the crater density increases in going from type 1 craters to type 2 craters and decreases from type 2 craters to type 5 craters. For the basin, the crater density decreases in going from type 1 craters to type 2 craters and increases from type 2 to type 3 craters. Type 3 craters are most abundant in the basin. The great number of craters with faults and the presence of craters with several terraces and craters with several terraces and faults in the mare region are probably related to crater degradation during the period

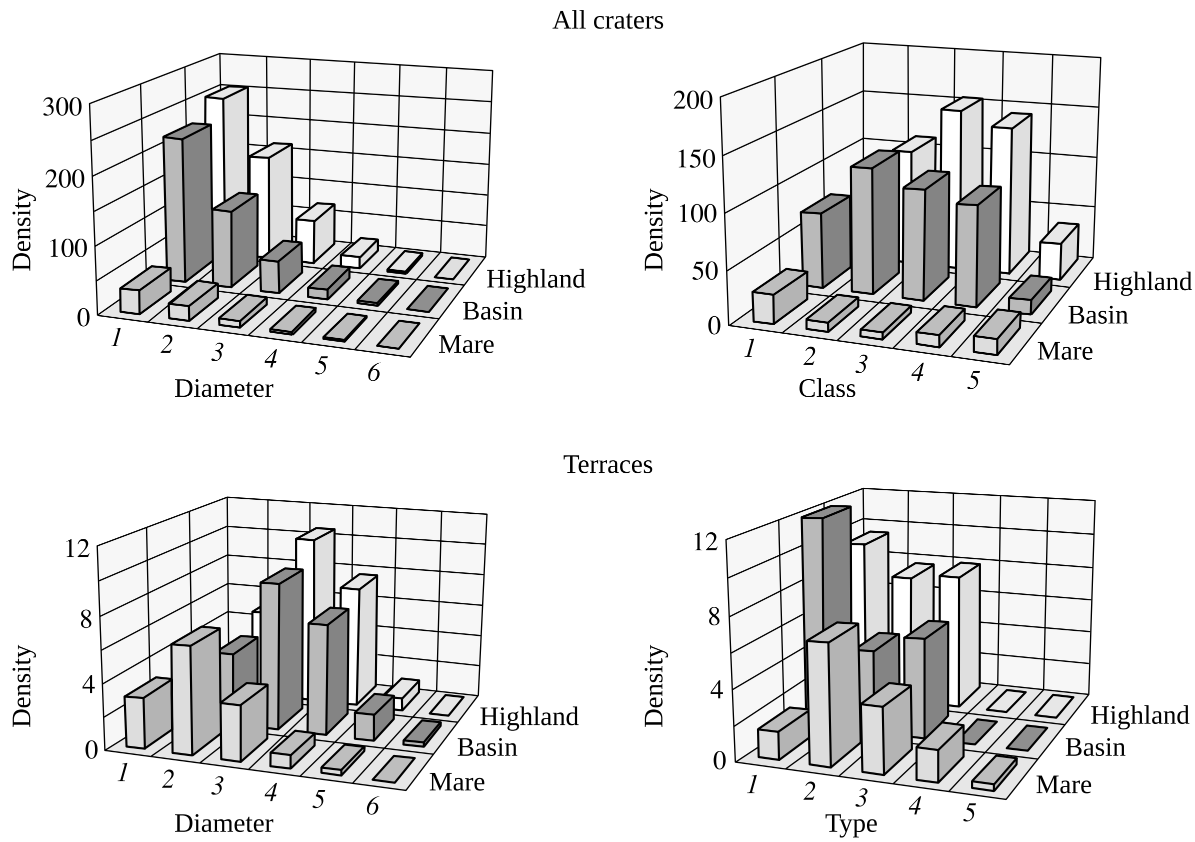

Fig. 4. Histograms showing the distributions of densities of craters (per 1 million km^2) with different diameters [(*1*) 10–20 km, (*2*) 20–40 km, (*3*) 40–80 km, (*4*) 80–160 km, (5) 160–320 km, and (*6*) 320–640 km]; degrees of rim degradation [(*1*) highly pronounced rim, (*2*) pronounced rim, (*3*) smoothed rim, (*4*) degraded rim, and (*5*) ruin]; and different types of inner-slope degradation [(*1*) one terrace, (*2*) one fault, (*3*) one terrace and one fault, (*4*) many terraces, and (*5*) many terraces and one fault] for the three regions studied.

of basaltic volcanism, whereas rare craters with one terrace are young, weakly degraded formations (Fig. 4).

Peaks, hills, and ridges. The distributions of craters are similar for the three regions studied: craters with many hills on the floor are most abundant, and craters with one peak and one hill on the floor and craters with many peaks and one hill are least abundant. Craters with ridges on the floor are lacking in all the regions studied. However, in the mare region, craters with many peaks on the floor are the second most abundant impact structures (Fig. 5).

Fissures and chains. The distributions of craters are also similar for the three regions studied: craters with one chain on the floor are most abundant, and craters with one chain and one fissure on the floor are least abundant. We found no craters with many chains on the floor or craters with one chain and many fissures in all the regions studied. Craters with one fissure and craters with one chain and one fissure are few in number both in the highland region and in the basin, and craters with several fissures are lacking in these regions (Fig. 5). Craters with one fissure on the floor are the second most abundant structures in the mare region. This is likely to be related to the peculiarities of endogenic processes in the regions of basaltic volcanism.

Character of the crater floor. The majority of craters in the South Pole–Aitken Basin and the highland region have rough floors, whereas about one-third of craters in the mare region have flat floors.

The presence of lavas on the crater floor. There are no craters with the floor completely flooded by lavas in the highland region and the basin; however, craters with the floor partly covered by lavas are present in these regions. The majority of craters in the mare region have lavas on the floor, a portion of the craters have their floors completely flooded by lavas.

The presence of ray systems. In the South Pole–Aitken Basin, we found no craters with the ray system. There are three craters with ray systems in the highland region, whereas eleven craters with ray systems are present in the mare region. Why craters with ray systems are lacking in the basin remains a mystery.

CONCLUSION

Our analysis revealed certain similarities and distinctions in the morphology of craters in the lunar

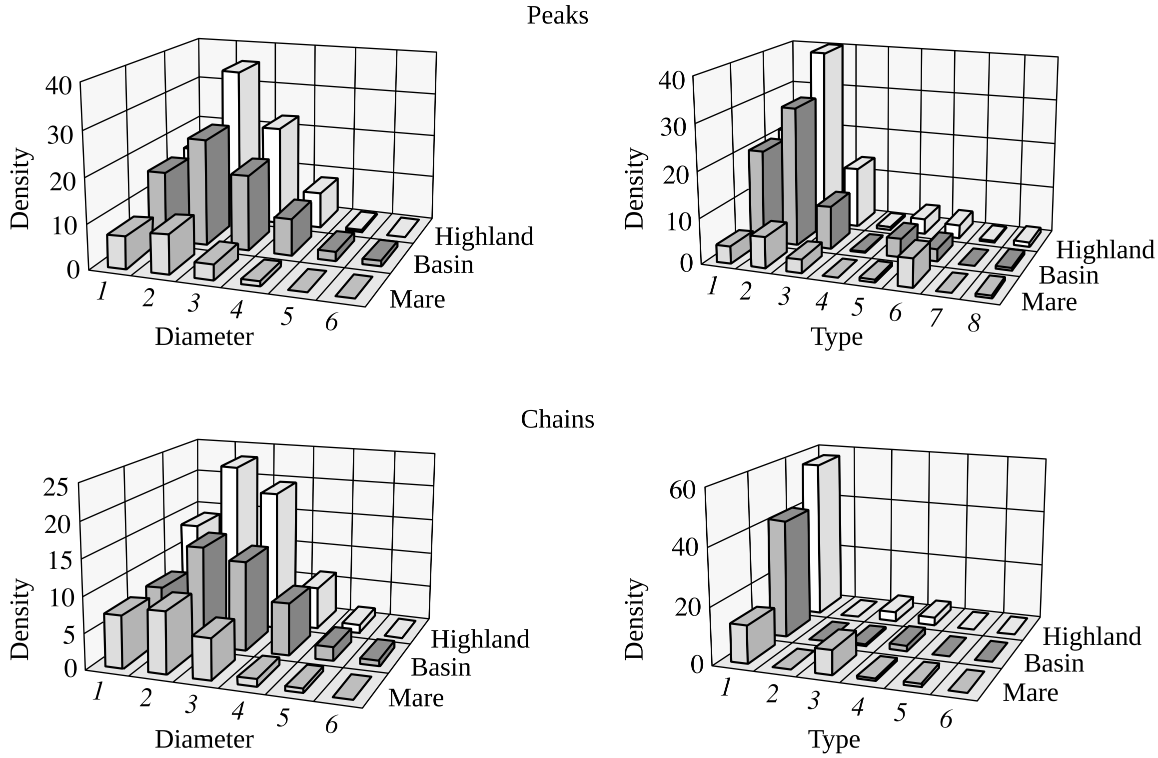

Fig. 5. Histograms showing the distributions of densities of craters (per 1 million km^2) with different diameters [(*1*) 10–20 km, (*2*) 20–40 km, (*3*) 40–80 km, (*4*) 80–160 km, (5) 160–320 km, and (*6*) 320–640 km]; peak types** [(*1*) one hill, (*2*) many hills, (*3*) one peak, (*4*) one peak and one hill, (*5*) one peak and many hills, (*6*) many peaks, (*7*) many peaks and one hill, and (*8*) many peaks and hills]; and fissures and chains of small craters [(*1*) one chain, (*2*) many chains, (*3*) one fissure, (*4*) one chain and one fissure, (*5*) many fissures, and (*6*) one chain and many fissures] for the three regions studied.

regions studied. Above all, these regions differ in the crater density: the density of craters in the highland region exceeds those in the South Pole–Aitken Basin and the mare region by factors of 1.2 and 6.9, respectively. This variation in the crater density is related to the various ages of the regions studied. The highland is the oldest lunar region. The basin is younger—this region was likely formed late in the period of heavy bombardment. Out of the regions under consideration, the mare region is the youngest one. It formed after the period of heavy bombardment.

The distributions of craters in the highland region and the basin are similar. The revealed dissimilarities (the predominance of highly degraded craters and craters with faults in the highland region) are related not only to the various ages of these regions but also to some tectonic processes, which did not proceed in the basin. As mentioned above, Vallis Snellius, Vallis Rheita, and Vallis Palitzsch intersect the highland region. Since not only craters with smoothed rims but craters with well pronounced rims are degraded in this region, we assume that the degradation processes proceeded a long time after the formation of this lunar region had been completed. We attribute the high density of craters with pronounced rim in the South Pole–Aitken Basin as compared to the highland to the younger age of the basin. The fact that the distribution of craters by morphological classes for the basin is similar to the mean distribution for the lunar highlands is not surprising, because the latter distribution represents the data averaged over 83% of the lunar surface. The morphology of craters in the mare region is found to differ drastically from those in the basin and the highland region. A low crater density and the abundance of crater-ruins and craters with faults in the mare region are due to lava flooding of ancient depressions during the period of basaltic volcanism and the destruction of the majority of craters formed in the preceding heavy-bombardment period. Note that most of the crater-ruins are observed in the regions adjacent to the mare–highland boundaries (Rodionova *et al.*, 1989b). The fact that the density of craters with smoothed rims, which are abundant in the highland region, is low in the mare region indicates that it is precisely craters of this class that disappeared during the lava filling of ancient depressions. However, we found distinctions in the crater morphology of the regions which cannot be explained by the different ages of the considered regions: the mare region differs in the densities of craters with fissures and chains of small craters, peaks, and lavas on the floor. We attribute these distinctions to the difference in endogenic processes that proceeded in the considered regions. The endogenic processes should reveal themselves more often in the mare regions, because the lunar crust here is much thinner than in the highland regions.

Hiesinger and Head (1999) advocate that the crustal thickness is a factor limiting the eruption of lunar basalts onto the surface. Rising magma erupts onto the surface in places with a thin crust. The maximum crustal thickness in the regions containing basalts is 50–60 km. On the farside, the crust is thicker; therefore, magma solidifies in dikes below the surface. In the South Pole–Aitken Basin, the crustal thickness is no more than 60 km and, in some places, only 30 km (Zuber *et al.*, 1994). However, basaltic lavas occupy only a small part of the basin, and the endogenic processes affected craters in the basin to the same extent as craters on the nearside. We assume that the above distinctions in the morphology of craters on the nearside are due to the higher endogenic activity on the lunar nearside caused by Earth's influence.

ACKNOWLEDGMENT

This work was supported through the Astronomy National Science and Technology Program, project no. 1.6.1.

REFERENCES

Basilevsky, A.T., Ivanov, B.A., Florenskii, K.P., *et al.*, *Udarnye kratery na Lune i planetakh* (Impact Craters on the Moon and Planets), Moscow: Nauka, 1983.

Binder, A.E., *Lunar Prospector Overview*, 1998, http://lunar.arc.nasa.gov.

Florensky, K.P., Basilevsky, A.T., and Grebennik, N.N., The Relationship between Lunar Craters Morphology and Crater Size, *Moon*, 1976, vol.16, no. 1, pp. 59–70.

Florenskii, K.P., Basilevsky, A.T., and Grebennik, N.N., The Morphology of Impact Craters on the Moon and Other Planets, in *Meteoritnye struktury na poverkhnosti planet* (Meteoritic Structures on the Planetary Surfaces), Moscow: Nauka, 1979.

Hartmann, W.K., Paleocratering of the Moon: Review of Post-Apollo Data, *Astrophys. Space Sci.*, 1972, vol. 17, pp. 48–64.

Hiesinger, H. and Head, J.W., Ages of Oceanus Procellarum Basalts and Other Nearside Mare Basalts, *Workshop on New Views of the Moon. II.* Understanding the Moon through the Integration of Diverse Datasets, *LPI Contrib.*, 1999, no. 980, pp. 27–28.

Khramchikhin, A.A., The Regularities in the Distribution of Lunar Craters as an Age Indicator of the Surface, *Astron. Vestn.*, 1994, vol. 28, no. 3, pp. 74–80.

Leikin, G.A. and Sanovich, A.H., Origin of the Southern Basin on the Far Side of the Moon, *Astron. Vestn.*, 1985, vol. 19, no. 2, pp. 113–119.

Rodionov, B.N., Isavnina, I.V., Avdeev, Yu.S., *et al.*, New Data on the Lunar Figure and Relief from the Photographs Obtained by *Zond-6, Kosm. Issled.*, 1971, vol. 9, no. 3, pp. 450–458.

Rodionov, B.N., Nefed'ev, A.A., Shpekin, M.I., *et al.*, The Relief of the Far Side of the Moon as Revealed from *Zond-6* Photographs, *Kosm. Issled.*, 1976, vol. 14, no. 4, pp. 624–629.

Rodionova, Zh.F., Karlov, A.A., Skobeleva, T.P., *et al.*, *Morfologicheskii katalog kraterov Luny* (Morphological Catalog of Lunar Craters), Moscow: Mosk. Gos. Univ., 1987.

Rodionova, Zh.F., Shevchenko, V.V., Karlov, A.A., *et al.*, An Analysis of Lunar Crater Distribution Based on the Morphological Catalog, *Astron. Vestn.*, 1989a, vol. 23, no. 1, pp. 50–59.

Rodionova, Zh.F., Shevchenko, V.V., Karlov, A.A., *et al.*, A Morphological Analysis of Cratering on the Moon, *Tr. Gos. Astron. Inst. im. Sternberga*, 1989b, vol. LXI, pp. 356–376.

Rodionova, J.F. and Khramchikhin, A.A., The Global Features of Cratering on the Moon and Mars, *Abstr. Lunar Planet. Sci. Conf. XXVII*, 1996, pp. 1091–1092.

Shoemaker, E.M., Robinson, M.S., and Eliason, E.M., The South Polar Region of the Moon as Seen by *Clementine*, *Science*, 1994, vol. 266, pp. 1851–1854.

Spudis, P.D., Reisse, R.A., and Gills, J.J., Ancient Multiring Basins on the Moon Revealed by *Clementine* Laser Altimetry, *Science*, 1994, vol. 266, pp. 1848–1851.

Wilhelms, D.E., *The Geologic History of the Moon*, US Geologic Survey, Professional Paper 1348, Washington: US Government Printing Office, 1987, pp. 143–155.

Zuber, M.T., Smith, D.E., Lemoine, F.G., *et al.*, The Shape and Internal Structure of the Moon from the *Clementine* Mission, *Science*, 1994, vol. 266, pp. 1839–1843.